This article has been accepted for publication in a future issue of this journal, but has not been fully edited. Content may change prior to final publication. Citation information: DOI 10.1109/TPWRS.2018.2877236, IEEE Transactions on Power Systems

Real-time Rolling Horizon Energy Management for the Energy-Hub-Coordinated Prosumer Community from a Cooperative Perspective

Li Ma, Nian Liu, *Member*, *IEEE*, Jianhua Zhang, *Member*, *IEEE*, Lingfeng Wang, *Senior Member*, *IEEE*

Abstract—The concept of energy hub (EH) was proposed to facilitate the synergies among different forms of energy carriers. Under the new electricity market environment, it is of great significance to build a win-win situation for prosumers and the hub manager (HM) at the community level without bringing extra burden to the utility grid. This paper proposes a cooperative trading mode for a community-level energy system (CES), which consists of the energy hub and PV prosumers with the automatic demand response (DR) capability. In the cooperative trading framework, a real-time rolling horizon energy management model is proposed based on cooperative game theory considering the stochastic characteristics of PV prosumers and the conditional value at risk (CVaR). The validity of the proposed model is analyzed through optimality proof of the grand coalition. A contribution-based profit distribution scheme and its stability proof are also provided. Moreover, in order to solve the optimization model, it is further transformed into a more easily resolved mixed integer linear programming (MILP) model by adding auxiliary variables. Finally, via a practical example, the effectiveness of the model is verified in terms of promoting local consumption of PV energy, increasing HM's profits, and reducing prosumers' costs, etc.

***Index Terms*—Energy Hub, PV prosumers, cooperative trading mode, cooperative game, CCHP, demand response, stochastic optimization.**

NOMENCLATURE

Sets:

$\boldsymbol{I}_{fi}$	Fixed load set of prosumer *i*.
$\boldsymbol{I}_{si}$	Shiftable load set of prosumer *i*.
$\boldsymbol{I}_{ti}$	Thermal demand set of prosumer *i*.
$\boldsymbol{P}_i$	PV output set of prosumer *i*.
$\boldsymbol{N}_{Li}$	Net load set of the prosumer *i*.
$\boldsymbol{p}_{gs}$	Electricity selling price set of the utility grid.
$\boldsymbol{p}_{gb}$	Electricity buying price set of the utility grid.
$\boldsymbol{p}_{ms}$	Electricity selling price set of the HM.
$\boldsymbol{p}_{mb}$	Electricity buying price set of the HM.
Ω	The scenario set in cooperative mode.
ω_m	*m*-th scenario of all the prosumers.

Parameters:

t	The time of current period.
η_{cchp}	Power generation efficiency of the microturbine.
η_{loss}	Heat loss coefficient in the CCHP system.
δ_{heat}	Heating coefficient of the waste heat boiler.
δ_{cool}	Cooling coefficient of the absorption refrigerator.
r_{heat}	Heating price of the HM.
r_{cool}	Cooling price of the HM.
P_M^t	Electricity price at period *t*.
P_{M,ω_m}^h	Electric price under the *m*-th scenario at period *h*.
β	Confidence level.
α	Value at risk of all the prosumers with β.
γ	Weight of the CVaR value.

Variables:

$[\alpha_i, \beta_i]$	Optional time range interval of prosumer *i*'s shiftable load.
Q_i	Prosumer *i*'s shiftable load demand.
l_{fi}^h	Fixed load of prosumer *i* at period *h*.
l_{si}^h	Shiftable load of prosumer *i* at period *h*.
P_i^h	PV output of prosumer *i* at period *h*.
N_{Li}^h	Net load of prosumer *i* at period *h*.
N_L^h	Total net load of all prosumers in the HM.
l_{ti}^h	The thermal demand of prosumer *i* at period *h*.
l_{hi}^h	Heat demand of prosumer *i* at period *h*.
l_{ci}^h	Cool demand of prosumer *i* at period *h*.
$p_{t\_cchp}^h$	The total thermal output of CCHP at period *h*
$p_{c\_cchp}^h$	The total cool output of CCHP at period *h*.
$p_{h\_cchp}^h$	Total heat output of CCHP at period *h*.
$p_{e\_cchp}^h$	Total electric output of CCHP at period *h*.
F_{tmi}^h	Thermal fee prosumer *i* pays to the HM at period *h*.
$C^{t\sim H}$	Overall cost of all the prosumers from period *t* to period *H*.
l_f^t	Fixed load of all the prosumers at period *t*.
l_s^t	Shiftable load of all the prosumers at period *t*.
P^t	PV output of all the prosumers at period *t*.
$\pi(\omega_m)$	Probability of the *m*-th scenario.
l_{f,ω_m}^h	Fixed load of all the prosumers at period *h* under the *m*-th scenario.
$P_{\omega_m}^h$	PV output of all the prosumers at period *h* under the *m*-th scenario.

This work was supported in part by the National Natural Science Foundation of China under Award 51877076, and in part by the U.S. National Science Foundation Industry/University Cooperative Research Center on Grid-connected Advanced Power Electronic Systems (GRAPES) under Award GR-17-14. (*Corresponding author: Nian Liu*).

L. Ma is with State Key Laboratory of Alternate Electrical Power System with Renewable Energy Sources, North China Electric Power University, Beijing 102206, China, and is also with the Department of Electrical Engineering and Computer Science, University of Wisconsin-Milwaukee, Milwaukee, WI 53211, USA (e-mail: ma27@uwm.edu).

N. Liu and J. Zhang are with State Key Laboratory of Alternate Electrical Power System with Renewable Energy Sources, North China Electric Power University, Beijing 102206, China (e-mail: nian_liu@163.com; jhzhang001@163.com).

L. Wang is with the Department of Electrical Engineering and Computer Science, University of Wisconsin-Milwaukee, Milwaukee, WI 53211, USA (e-mail: l.f.wang@ieee.org).

This article has been accepted for publication in a future issue of this journal, but has not been fully edited. Content may change prior to final publication. Citation information: DOI 10.1109/TPWRS.2018.2877236, IEEE Transactions on Power Systems

l_{s}^{h} Shiftable load of all prosumers at period h.
$u(\omega_m)$ An auxiliary variable of the scenario ω_m.
$F_{\mathrm{tm}}^{t\sim H}$ Thermal fee all the prosumers paid to the HM from period t to period H.
$l_{\mathrm{s\_opt}}^{h}$ Optimized result of l_{s}^{h}.
$C_{\mathcal{N}/i}^{t\sim H}(\mathrm{CO})$ Total cost of prosumers' coalition except for prosumer i.
$E_{\mathrm{add}}^{t\sim H}$ The added profit of cooperative trading mode compared to non-cooperative one.
$E_{\mathrm{add\_}i}^{t\sim H}$ Prosumer i's contribution to the profit.
ρ_i Contribution weight of prosumer i.
E_{m}^{t} HM's profit at period t.
$E_{\mathrm{m},\omega_m}^{h}$ HM's profit at period h in the scenario ω_m.
$E_{\mathrm{m}}^{t\sim H}(\mathrm{CO})$ The HM's profit from period t to period H.

I. Introduction

Concerns on environmental problems and energy supply security have arisen over the past decades due to the fast dwindling natural resources and the rapid increase of fossil fuels demand. Meanwhile, the interactions among different energy carriers have been growing with the increasing utilization of renewable energy resources (RES), distributed generation (DG), and combined cooling, heating and power generation (CCHP) technologies [1].

Traditionally, the energy carriers such as electricity and natural gas systems were designed, planned, and operated independently. In order to study the interactions between them, new concepts and tools are required. The concept of 'Energy Hub' (EH) has been proposed to model the integration of different energy carriers efficiently. An EH is defined as a node within an electric power system, in which exchange of energy and information among energy sources, loads, and the external systems take place [2]. EH obtains various forms of energy carriers at the input terminals that are connected to the energy infrastructures, and supplies the demand at the output terminals [1]. For a single EH, it could range from the aggregation of energy sources and loads at the customer level to the aggregation of distributed energy resources and customer cluster [3], and it can even be extended to an entire city.

As an important component of the EH, CCHP systems are deemed to be highly promising in the future energy portfolio for their high efficiency and low emissions characteristics [4] as they generate electric and thermal energy simultaneously. There are two typical simple strategies for CCHPs, i.e., following the electric load and following the thermal load [5]. In addition, more complex optimal strategies are studied, where the operating cost or emissions are minimized [6] according to some external signals. The micro-turbines have been extensively used in the small-scale CCHP systems (20 kW–1MW), which have the most active and mature market [4, 7] and can be applied at the community level.

In the near future, it is expected that the number of geographically dispersed EHs connected to energy networks will increase remarkably. There have been some studies related to EHs thus far. An optimally designed and sized model was proposed for a system of interconnected hubs considering economic and technical aspects [8]. Financial analyses for energy hubs' investment were carried out in [9, 10]. In terms of operation optimization, there have been several studies for industrial and residential EHs. An optimal industrial load management (OILM) model, which can be embedded in an EH management system for any industrial users, was proposed in [2]. The optimal operation of residential EH was studied in [11, 12]. For the real-time energy management of EHs, mathematical optimization models were proposed under a real-time framework in [12], which can be used to optimally control major residential energy loads, storage and production components considering the customers' comfort level. In [13], an EH operation-scheduling scheme in the presence of data uncertainty was studied based on an affine arithmetic methodology, which is able to address the real-time EH operation-scheduling problem. A real-time scheduling problem of EHs in a dynamic pricing market was modeled as an exact potential game in [14].

From the viewpoint of the demand side, several significant changes have also been taking place in recent years. On the one hand, in order to make power systems more environmentally friendly, renewable energy resources such as PV panels are being more commonly utilized [15]. In addition, advanced two-way communication network and information technologies are being integrated to provide imperative facilities for enabling demand response (DR) programs. Developments of customer-owned DGs and DR programs are transforming the traditional consumers to the so-called prosumers, who can produce electricity or adjust load demand (reducing load on the demand side is analogous to producing power on the generation side). On the other hand, electricity market reform on the demand side has allowed the new operation entities to serve as electricity retailers, which has broken the traditional market monopoly situation of electric power companies. Under this new electricity market environment, the EHs will play an even greater role in the whole energy ecosystem, e.g., the Hub manager (HM) can also trade energy directly with the connected prosumers.

In these circumstances, it is of great significance to build a win-win situation for prosumers and HM without bringing extra burden to the construction and operation of the utility grid. To this end, this paper proposes a cooperative trading mode framework for the community-level energy system (CES) consisting of the energy hub and multiple PV prosumers connected to it. In this proposed trading mode, the prosumers can share the electric energy with each other, while the HM's CCHP electric production can also be sold to the prosumers directly with more favorable prices which can even be equal to the utility grid's selling prices, rather than being sold to the utility grid with the utility grid's buying prices like what was commonly done in the past. Then both HM and prosumer cluster will obtain extra profits because the utility grid selling prices are higher than the buying prices in most cases, and they will also be inclined to share more energy to the others, which will further promote the local consumption of renewable energy. As a fundamental energy unit, community-level energy hub (CEH) related research will be needed for developing the whole integrated energy system. In the long term, the cooperative trading mode framework for the CESs will be important, in terms of improving

This article has been accepted for publication in a future issue of this journal, but has not been fully edited. Content may change prior to final publication. Citation information: DOI 10.1109/TPWRS.2018.2877236, IEEE Transactions on Power Systems

energy efficiency, facilitating the integration and local consumption of distributed energy, reducing system power losses and pollutant emissions, and increasing the reliability of energy supply.

As an important and promising method to solve the cooperative problems, the cooperative game has been already utilized in handling several challenging problems in smart grid. In [16], the game-theoretic coalition formulation strategy for reducing power loss in microgrids was proposed. In [17], a direct electricity trading model in smart grid was proposed with a coalitional game scheme. In [18], an online air-conditioning energy management model was studied under the coalitional game framework. However, the stochastic characteristics of certain parameters in the smart grid have been rarely considered in the relevant literature.

Overall, the major contributions of this paper are listed as follows:

1) The cooperative trading mode framework for the CES is proposed, considering the energy interactions between HM and prosumers, and power-sharing between prosumers.

2) The real-time rolling horizon energy management optimization model for the CES is proposed from the viewpoint of the cooperative game considering the parameters' stochastic characteristics, and the CVaR value is also integrated into the objective function.

3) The validity of the proposed energy management optimization model is analyzed through optimality proof of the grand coalition. The corresponding profit distribution method based on the prosumers' contribution and the associated stability proof are also studied.

4) The equivalent method of the proposed nonlinear optimization model is introduced. The multi-scenario optimization model with a segmented objective function is transformed into a mixed integer linear optimization problem which can be easily solved.

II. Structure and Trading Model of CES

A. The Structure of the CES

The system architecture of the CES in this paper is shown in Fig. 1. There are two kinds of inputs: electricity and natural gas. The bi-directional communications between the HM and PV prosumers are also deployed in the CES.

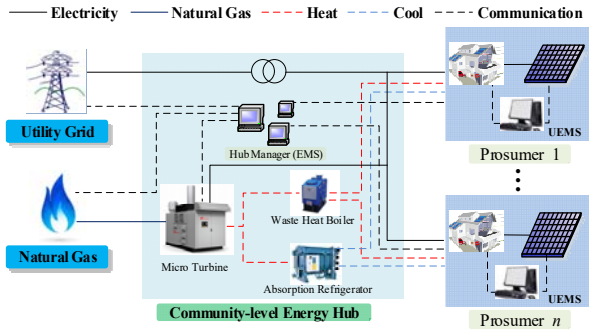

Fig. 1. The system structure of the CEH.

The CEH consists of a Hub Manager (HM), transformers, and a CCHP system composed of microturbines, waste heat boilers, and absorption refrigerators. The CEH is responsible for supplying various energies to the connected prosumers and the energy balance of CES. The HM is also in charge of the interoperability among all participants, and it can be seen as the energy management executor of the CES.

Each prosumer consists of PV sources, loads, smart meters, user energy management system (UEMS), etc. The UEMS is employed to gather data of the PV source, electric load, and thermal load, as well as to receive information or instructions from the HM. In addition, the UEMS is in charge of controlling and optimizing the prosumers' energy consumption. Due to the intermittent nature of PV sources, a PV output forecasting function [19] should also be considered in the UEMS.

B. Cooperative Trading Mode for the CES

As mentioned before, we apply a trading mode from the cooperative perspective in this paper. The schematic diagram of the cooperative trading mode for the CES is shown in Fig. 2.

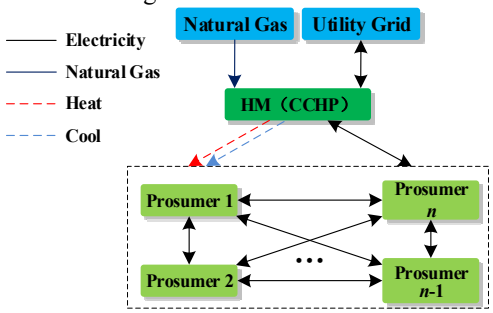

Fig. 2. Schematic diagram of the cooperative trading mode.

The cooperative trading mode involves two kinds of cooperation. The first one is the cooperation between HM and prosumers. Traditionally, the CCHP's electric power was not allowed to be sold to consumers directly but could only be purchased by the utility grid with its buying prices in countries such as China. The cooperative trading mode in Fig. 2 is proposed based on the new market environment, so the electric output of the CCHP can be sold to the prosumers at first with more favorable prices, and then be sold back to the grid if there is redundant power. In order to sell CCHP output electricity to the prosumers with beneficial prices, the HM should manage to attract the prosumers trading with it rather than the utility grid.

One way to attract prosumers is to facilitate the PV output sharing between the prosumers, which is the second kind of cooperation, and HM can play the role of a coordinator in this process. Although PV output curves have high similarity inside a community due to the almost same solar radiation, the net loads vary widely among PV prosumers possessing different load profiles and PV capacities [20]. Complementary characteristics of different net loads make it possible to share the PV outputs between prosumers, which is almost at no cost. This kind of power sharing will reduce electricity purchases from the utility grid, and then save the total cost for the prosumer cluster. In order to facilitate the PV output sharing, a coordinator is required, and the HM is an appropriate candidate. As a coordinator, the HM can trade energy with its proxied prosumers directly and benefit from that, and the HM is also responsible for the allocation of cost savings between the prosumers. Considering the PV output sharing, if the PV sources still cannot meet the load demands of the prosumers,

This article has been accepted for publication in a future issue of this journal, but has not been fully edited. Content may change prior to final publication. Citation information: DOI 10.1109/TPWRS.2018.2877236, IEEE Transactions on Power Systems

they will purchase electricity from the HM (i.e., from CCHP electric power first, and then from the utility grid). On the other hand, if the demand of prosumers is less than the PV sources' output, the surplus PV power will be sold back to the utility grid through the HM.

According to the above description, even the HM sets its prices to be the same as the utility prices, both HM and prosumers will profit from the cooperative trading mode. If the HM desires more solid cooperation with the prosumers, it can also devise alternative selling pricing plans which are more appealing to the prosumers. Considering the automatic DR capability of the prosumers, the optimization model for CES energy management under the cooperative trading mode is studied in the following section.

III. Optimization Model for Energy Management

A. The Basic Model of the CES

1) Electric load requirements of the prosumer

In this study, prosumers have two kinds of loads, i.e., fixed loads and shiftable loads. Furthermore, the PV power will counteract the prosumer's load.

a) Fixed load

It is necessary to guarantee the power supply for the fixed loads, such as lights, refrigerators, televisions, elevators, etc., to ensure the daily-life convenience. The fixed load set of prosumer i within a fixed period is defined as:

$$\boldsymbol{l}_{\mathrm{fi}} \triangleq [l_{\mathrm{fi}}^{1},\ldots,l_{\mathrm{fi}}^{H}], \quad i=1,2,\ldots,n \tag{1}$$

where n is the total number of prosumers in the cluster, and H is the length of time horizon, which is 24 hours in this study.

b) Shiftable loads

For shiftable loads, consumers can modify the service time according to the electricity prices and other information or preferences. The shiftable load set of prosumer i within a fixed period is defined as:

$$\boldsymbol{l}_{si} \triangleq [l_{si}^{1},\ldots,l_{si}^{H}], \quad i=1,2,\ldots,n \tag{2}$$

Assuming the number of the shiftable loads of prosumer i is K_i, the shiftable load value of prosumer i at period h is the sum of all its shiftable loads:

$$l_{si}^{h}=\sum_{k=1}^{K_i} l_{sik}^{h} \tag{3}$$

where l_{sik}^{h} is the shiftable load k of prosumer i at period h. The shiftable load can be further divided into two categories: non-interruptible shiftable load and interruptible shiftable load.

- The non-interruptible shiftable loads must be fulfilled without interruption to avoid efficiency losses. They may include washers, dishwashers, dryers, etc. The detailed model for a non-interruptible shiftable load can be expressed as:

$$\begin{cases} l_{sik}^{h} = p_{ik}, & h\in[t_{ik},t_{ik}+\Delta T_{ik}] \\ l_{sik}^{h} = 0, & h\notin[t_{ik},t_{ik}+\Delta T_{ik}] \end{cases} \tag{4}$$

$$[t_{ik},t_{ik}+\Delta T_{ik}]\in[\alpha_{ik},\beta_{ik}] \tag{5}$$

$$\sum_{h=t_{ik}}^{t_{ik}+\Delta T_{ik}} l_{sik}^{h} = Q_{ik} \tag{6}$$

where p_{ik} is the electric power of shiftable load k for prosumer i (the shiftable loads are assumed to be constant-power in this paper), t_{ik} is the start time of the shiftable load k, ΔT_{ik} is the duration time of the shiftable load k, $[\alpha_{ik},\beta_{ik}]$ is the optional time range interval of the shiftable load k, and Q_{ik} is the demand amount of the shiftable load k, which is the sum of all power consumption of every period.

- The interruptible shiftable loads need not to be fulfilled continuously, which can be divided into several tasks in multiple time periods. Plug-in hybrid electric vehicles (PHEVs) are a typical example of interruptible shiftable loads. The detailed model for an interruptible shiftable load can be expressed as follows:

$$\begin{cases} l_{sik}^{h} = p_{ik}, & h=t_{ik1},t_{ik2},\cdots,t_{ikJ_{ik}} \\ l_{sik}^{h} = 0, & h\neq t_{ik1},t_{ik2},\cdots,t_{ikJ_{ik}} \end{cases} \tag{7}$$

$$t_{ik1}<t_{ik2}<\cdots<t_{ikJ_{ik}} \tag{8}$$

$$t_{ikj}\in[\alpha_{ik},\beta_{ik}], \quad j=1,2,\cdots,J_{ik} \tag{9}$$

$$\sum_{h=t_{ik1},t_{ik2},\cdots,t_{ikJ_{ik}}} l_{sik}^{h} = Q_{ik} \tag{10}$$

where J_{ik} is the total task number of the shiftable load k for prosumer i, t_{ikj} is the start time of task j. It is assumed that each task lasts for one hour here. The expression (8) means that each task has to be carried out in sequence.

According to the expressions (4)-(10), the shiftable load model is discrete, so we transform it into a continuous one by adopting the method proposed in [21], which is defined as:

$$\begin{cases} l_{si}^{h\_\min} < l_{si}^{h} < l_{si}^{h\_\max}, & h\in[\alpha_i,\beta_i] \\ l_{si}^{h} = 0, & h\notin[\alpha_i,\beta_i] \end{cases} \tag{11}$$

$$\sum_{h=1}^{H} l_{si}^{h} = Q_i \tag{12}$$

In these expressions, l_{si}^{h} is treated as a continuous variable within the interval $[l_{si}^{h\_\min}, l_{si}^{h\_\max}]$, whose upper bound and lower bound can be determined by the Monte Carlo method [21]. The start time of each shiftable appliance can be determined in turn based on the results of $[l_{si}^{1},\ldots,l_{si}^{H}]$.

2) Thermal load requirements of the prosumer

The heating and cooling resources produced by CCHPs would be utilized to meet the prosumers' thermal demand. A customer's thermal demand often consists of hot water and low-pressure steam in winter, and the hot water and cooling demand in summer. The thermal demand set of prosumer i within a fixed period is defined as:

$$\boldsymbol{l}_{ti} \triangleq [l_{ti}^{1},\ldots,l_{ti}^{H}], \quad i=1,2,\ldots,n \tag{13}$$

where l_{ti}^{h} is composed of heat demand and cooling demand of prosumer i at period h:

$$l_{ti}^{h} = l_{\mathrm{hi}}^{h} + l_{ci}^{h} \tag{14}$$

3) Power production of the prosumer's PV

A PV cell's produced power usually changes with solar intensity and ambient temperature. However, there is only one maximum power point (MPP) in a specific condition. The maximum power point tracking (MPPT) strategy is always applied to ensure PV modules work at MPPs in a changing environment. The predicted value of the PV source's active power of prosumer i within a fixed period is defined as:

$$\boldsymbol{P}_i = [P_i^{1},\ldots,P_i^{H}], \quad i=1,2,\ldots,n \tag{15}$$

4) Model of the CCHP system

The model of the CCHP system consists of two parts, i.e., thermal energy and electrical energy [22].

$$p_{\mathrm{t\_cchp}}^{h} = p_{\mathrm{c\_cchp}}^{h} + p_{\mathrm{h\_cchp}}^{h} \tag{16}$$

$$p_{\mathrm{c\_cchp}}^{h} = \sum_{i=1}^{n} l_{ci}^{h}, \quad p_{\mathrm{h\_cchp}}^{h} = \sum_{i=1}^{n} l_{\mathrm{hi}}^{h} \tag{17}$$

where $p_{\mathrm{t\_cchp}}^{h}$ is the total thermal output of CCHP system at

This article has been accepted for publication in a future issue of this journal, but has not been fully edited. Content may change prior to final publication. Citation information: DOI 10.1109/TPWRS.2018.2877236, IEEE Transactions on Power Systems

period h, and $p^h_{\text{e\_cchp}}$ is the total electric output of CCHP at period h. The feasible region for a micro-turbine can be specified with a linear equation and has two extreme points at the minimum and maximum power productions according to [7]. Then $p^h_{\text{e\_cchp}}$ can be determined according to the strategy of following the thermal load [23] - it is usually applied from the industry point of view by the following relationship:

$$p^h_{\text{e\_cchp}} = \left(\frac{\sum_{i=1}^{n} l^h_{\text{hi}}}{\delta_{\text{heat}}} + \frac{\sum_{i=1}^{n} l^h_{\text{ci}}}{\delta_{\text{cool}}} \right) \cdot \frac{\eta_{\text{cchp}}}{1-\eta_{\text{cchp}}-\eta_{\text{loss}}} \tag{18}$$

The cost of the CCHP system can be defined as C^h_{cchp} [22]:

$$C^h_{\text{cchp}} = \left(\frac{p_{\text{gas}}}{L}\right) \cdot \left(\frac{p^h_{\text{e\_cchp}}}{\eta_{\text{cchp}}}\right) \tag{19}$$

where p_{gas} is the price of natural gas; and L is the low heating value of natural gas.

5) Model of system electric load

The net load of prosumer i at period h is determined by its fixed load, shiftable load, and PV output, which is defined as:

$$N^h_{\text{L}i} = l^h_{\text{fi}} + l^h_{\text{si}} - P^h_i \tag{20}$$

$$\boldsymbol{N}_{\text{L}i} = \left[N^1_{\text{L}i}, N^2_{\text{L}i}, \ldots, N^H_{\text{L}i} \right], \quad i=1,2,\ldots,n \tag{21}$$

Regarding all the prosumers in the community as a system, the system net load at period h is:

$$N^h_{\text{L}} = \sum_{i=1}^{n} N^h_{\text{L}i} \tag{22}$$

B. Energy Management Optimization Model under the Cooperative Trading

1) Objective function of the optimization problem

Four components are considered in the objective function of the real-time rolling horizon energy management optimization model. As the shiftable load arrangement at the current period will influence the future arrangement, the cost at the current period and the costs in the future should be considered comprehensively. Additionally, we also consider the conditional value at risk (CVaR) [24] of the future costs, which represents the average value of the risk costs exceeding a certain confidence level. The fourth part is the thermal cost paid to the HM. In conclusion, the objective function of the optimization model can be defined as:

$$\begin{aligned} \textbf{min} \quad C^{t\sim H} &= P^t_{\text{M}} \cdot \left(l^t_{\text{f}} + l^t_{\text{s}} - P^t \right) \\ &+ \sum_{\omega_m \in \Omega} \left\{ \pi(\omega_m) \cdot \sum_{h=t+1}^{H} \left[P^h_{M,\omega_m} \cdot \left(l^h_{\text{f},\omega_m} + l^h_{\text{s}} - P^h_{\omega_m} \right) \right] \right\} \\ &+ \gamma \cdot \left[\alpha + \frac{1}{1-\beta} \cdot \sum_{\omega_m \in \Omega} \pi(\omega_m) \cdot u(\omega_m) \right] + F^{t\sim H}_{\text{tm}} \end{aligned} \tag{23}$$

where the four terms denote electricity cost in the current period, the sum of electricity costs in future periods, CVaR value, and total thermal cost, respectively.

$$F^{t\sim H}_{\text{tm}} = \sum_{h=t}^{H} \left(\sum_{i=1}^{n} r_{\text{heat}} \cdot l^h_{\text{hi}} + \sum_{i=1}^{n} r_{\text{cool}} \cdot l^h_{\text{ci}} \right) \tag{24}$$

Ω, which considers M scenarios, can be defined as:

$$\Omega \triangleq \left[\omega_1, \cdots, \omega_m, \cdots, \omega_M \right] \tag{25}$$

In this paper, the electricity prices that the HM supplies to the prosumers are the same as the utility grid's prices, which can be defined as:

$$\boldsymbol{p}_{\text{ms}} = \boldsymbol{p}_{\text{gs}}, \quad \boldsymbol{p}_{\text{mb}} = \boldsymbol{p}_{\text{gb}} \tag{26}$$

The relationship between HM's prices and P^t_M or P^h_{M,ω_m} can be expressed as follows:

$$\begin{aligned} P^t_M &= \begin{cases} p^t_{\text{ms}} & , l^t_{\text{f}} + l^t_{\text{s}} - P^t \geq 0 \\ p^t_{\text{mb}} & , l^t_{\text{f}} + l^t_{\text{s}} - P^t < 0 \end{cases}, \\ P^h_{M,\omega_m} &= \begin{cases} p^h_{\text{ms}} & , l^h_{\text{f},\omega_m} + l^h_{\text{s}} - P^h_{\omega_m} \geq 0 \\ p^h_{\text{mb}} & , l^h_{\text{f},\omega_m} + l^h_{\text{s}} - P^h_{\omega_m} < 0 \end{cases} \end{aligned} \tag{27}$$

The optimization variables in the above optimization model are l^t_{s} and l^h_{s} $(h = t+1, \ldots, H)$. The optimized result is defined as $C^{t\sim H}(\text{CO})$, i.e., the optimum comprehensive cost of all the prosumers in the cooperative trading mode.

2) Constraints of the optimization problem

It is assumed that the gas transmission capacity is satisfied in this paper, and then the constraints are due to two aspects. The first one is the constraints of shiftable loads, which are expressed in (28). The shiftable load bounds are determined by all prosumers' bounds. In addition, in order to avoid the upgrade of the utility grid, the shiftable load's corresponding system net load should not exceed the maximum value prior to optimization (expressed as $N^{\max}_{\text{L}}$). The second one is related to the CVaR [24], which is shown in (29).

$$\begin{aligned} \textbf{s.t.}1 \quad & l^{h\_\min}_{\text{s}} < l^h_{\text{s}} < l^{h\_\max}_{\text{s}}, h \in \left(\bigcup_{i=1}^{n} [\alpha_i, \beta_i] \right) \\ & l^{h\_\min}_{\text{s}} = \sum_{i=1}^{n} l^{h\_\min}_{si} \\ & l^{h\_\max}_{\text{s}} = \min\left(\sum_{i=1}^{n} l^{h\_\max}_{si}, N^{\max}_{\text{L}} + \sum_{i=1}^{n} \left(P^h_i - l^h_{\text{fi}} \right) \right) \\ & l^h_{\text{s}} = 0 \qquad\qquad , h \notin \left(\bigcup_{i=1}^{n} [\alpha_i, \beta_i] \right) \\ & \sum_{h=t}^{H} l^h_{\text{s}} = \sum_{i=1}^{n} Q_i - \sum_{h=1}^{t-1} l^h_{\text{s\_opt}} \end{aligned} \tag{28}$$

$$\begin{aligned} \textbf{s.t.}2 \quad & u(\omega_m) \geq 0 \\ & -\sum_{h=t+1}^{H} \left[P^h_{M,\omega_m} \cdot \left(l^h_{\text{f},\omega_m} + l^h_{\text{s}} - P^h_{\omega_m} \right) \right] + \alpha + u(\omega_m) \geq 0 \end{aligned} \tag{29}$$

where $u(\omega_m)$ is the auxiliary variable applied in the calculation of CVaR. The constraint (29) means the scenario cost which is greater than α (VaR value with β) will be used to calculate the CVaR value.

3) The benchmark optimization model

Traditionally, the prosumer or consumer usually trades electricity with the utility grid directly as an individual under normal circumstances (i.e., without an EH and HM) while its thermal load can be similarly supplied by CCHP system, which sells electricity directly to the utility grid. We regard this kind of traditional trading mode as a non-cooperative one.

Here, we use an associated optimization model under a non-cooperative trading mode as a benchmark (as introduced in **Appendix A**). The benchmark model has the similar objective function and constraints to the model under the cooperative trading mode. However, their service customers are different, as the former aims at the individual prosumer while the latter aims at all the prosumers in the community. For prosumer i, the corresponding optimized result under a non-cooperative trading mode is denoted as $C^{t\sim H}_i(\text{NC})$.

In the following sections, for brevity we will use **cooperative mode (with DR)** and **non-cooperative mode (with DR)** to represent the energy management optimization models under the cooperative trading mode and non-cooperative trading mode, respectively. These two models are operated by HM and UEMSs respectively.

This article has been accepted for publication in a future issue of this journal, but has not been fully edited. Content may change prior to final publication. Citation information: DOI 10.1109/TPWRS.2018.2877236, IEEE Transactions on Power Systems

IV. Profit Allocation and Load Determination

A. The Optimality Proof of the Grand Coalition

In the cooperative mode (with DR), we only consider the situation of the grand coalition, which means all the prosumers in the community form only one union. The optimality of the grand coalition will be proven based on the following theorem:

Theorem 1: When the value function is superadditive, forming the grand coalition is optimal for the maximization of the value function [25].

The superadditivity is defined as follows:

Definition 1: A value function is superadditive if for all disjoint sets $\mathcal{N}_1$ and $\mathcal{N}_2$, $V(\mathcal{N}_1 \cup \mathcal{N}_2) \geq V(\mathcal{N}_1) + V(\mathcal{N}_2)$.

Now we analyze the characteristic of the objective function in the optimization model (expression (23)), which is the cost of all prosumers.

For the first term of the objective function, it is the electricity purchasing cost at the current period, and the schematic diagram is shown in Fig. 3.

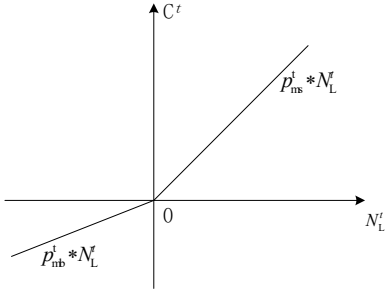

Fig. 3. Schematic diagram of electricity purchasing cost at period *t*.

As depicted in Fig. 3, because $p^t_{\mathrm{mb}} < p^t_{\mathrm{ms}}$, the electricity purchasing cost at period *t* is a convex function. For any N^t_{La} and N^t_{Lb}, the following relationship is satisfied:

$$C^t\left(N^t_{\mathrm{La}} + N^t_{\mathrm{Lb}}\right) \leq C^t\left(N^t_{\mathrm{La}}\right) + C^t\left(N^t_{\mathrm{Lb}}\right) \tag{30}$$

And for all disjoint sets $\mathcal{N}_1$ and $\mathcal{N}_2$,

$$C^t\left(\mathcal{N}_1 \cup \mathcal{N}_2\right) \leq C^t\left(\mathcal{N}_1\right) + C^t\left(\mathcal{N}_2\right). \tag{31}$$

As the second term of the objective function is a weighted sum of the electricity purchasing costs, its characteristic is similar to the first part.

For the third term of the objective function, according to the characteristic of CVaR, it also satisfies

$$C_{\mathrm{CVaR}}\left(\mathcal{N}_1 \cup \mathcal{N}_2\right) \leq C_{\mathrm{CVaR}}\left(\mathcal{N}_1\right) + C_{\mathrm{CVaR}}\left(\mathcal{N}_2\right) \tag{32}$$

From the above analysis, for the corresponding value function of $C^{t\sim H}$, i.e., $-C^{t\sim H}$ the following relationship is satisfied:

$$-C^{t\sim H}\left(\mathcal{N}_1 \cup \mathcal{N}_2\right) \geq \left[-C^{t\sim H}\left(\mathcal{N}_1\right)\right] + \left[-C^{t\sim H}\left(\mathcal{N}_2\right)\right] \tag{33}$$

Actually, the cost in the cooperative mode (DR) is the optimized result of (23). Taking any disjoint sets $\mathcal{N}_1$ and $\mathcal{N}_2$ as an example, the ultimate value corresponding to the optimized result must be greater than or equal to $-C^{t\sim H}(\mathcal{N}_1 \cup \mathcal{N}_2)$, and it is also greater than or equal to $[-C^{t\sim H}(\mathcal{N}_1)] + [-C^{t\sim H}(\mathcal{N}_2)]$.

Therefore, according to **Theorem 1**, the grand coalition is the optimal form for all the prosumers in the community under the cooperative mode (with DR).

B. The Profit Allocation of the Grand Coalition

With the grand coalition, the profit allocation issue also exists and is of high importance. If the profit distribution is not appropriate, there is a possibility that the prosumers would secede from the coalition. The Shapley value is a frequently used method for the profit allocation in the cooperative games [26], and it can reflect the participants' contribution in the cooperation. However it will be computationally complex and time-consuming when there are a number of participants. In view of this, we propose a simplified profit allocation method based on the contribution of each prosumer's participation, which will be realized by the HM.

Compared to the non-cooperative mode (with DR), the added profit of the cooperative mode (with DR) can be defined as:

$$E^{t\sim H}_{\mathrm{add}} = \left(-C^{t\sim H}\left(\mathrm{CO}\right)\right) - \sum_{i=1}^{n}\left(-C_i^{t\sim H}\left(\mathrm{NC}\right)\right) \tag{34}$$

For prosumer *i*, the contribution of its participation to the profit can be represented as:

$$E^{t\sim H}_{\mathrm{add}\_i} = \left(-C^{t\sim H}\left(\mathrm{CO}\right)\right) - \left[\left(-C^{t\sim H}_{\mathcal{N}/i}\left(\mathrm{CO}\right)\right) + \left(-C_i^{t\sim H}\left(\mathrm{NC}\right)\right)\right] \tag{35}$$

where $C^{t\sim H}_{\mathcal{N}/i}(\mathrm{CO})$ is the total cost of prosumers' coalition except prosumer *i*. Another cooperative mode (with DR) except for prosumer *i* needs to be established, which is similar to expressions (23)-(27).

According to the part A in this section, the value function in the cooperative mode (with DR) is superadditive, so $E^{t\sim H}_{\mathrm{add}\_i}$ must be greater than or equal to zero. We define the weight ρ_i of prosumer *i* based on its contribution to the coalition:

$$\rho_i = \frac{E^{t\sim H}_{\mathrm{add}\_i}}{\sum_{i=1}^{n} E^{t\sim H}_{\mathrm{add}\_i}} \tag{36}$$

Then the profit gained by prosumer *i* in the cooperative mode (with DR) can be represented as:

$$E_i^{t\sim H}\left(\mathrm{CO}\right) = \left(-C_i^{t\sim H}\left(\mathrm{NC}\right)\right) + \rho_i \cdot E^{t\sim H}_{\mathrm{add}\_i} \tag{37}$$

The stability of this allocation scheme is demonstrated in the next part through proving that the profit allocation is in the core of the cooperative game.

C. The Stability Proof of Profit Allocation

The core is the feasible allocation of profit which cannot be further improved by dividing the coalition into subsets. Its definition is as follows:

Definition 2: Let $\boldsymbol{x}$ be a profit vector which represents the profit that each player of the game achieves, and $\boldsymbol{x}_i$ be an element of $\boldsymbol{x}$, i.e., the profit of player *i*. Then, the core of the game, C_{core}, is defined as [25]:

$$C_{\mathrm{core}} = \left\{ \begin{array}{l} \boldsymbol{x} \in \mathbb{R}^{|\mathcal{N}|} : \sum_{i\in\mathcal{N}} x_i = V\left(\mathcal{N}\right) \\ \qquad \text{and} \sum_{i\in\mathcal{N}'} x_i \geq V\left(\mathcal{N}'\right), \forall \mathcal{N}' \subseteq \mathcal{N} \end{array} \right\} \tag{38}$$

Firstly, for the subsets $(\{1\},\{2\},\{3\},\ldots,\{n\})$, where each prosumer acts in the non-cooperative mode (with DR), the prosumer *i*'s profit is $C_i^{t\sim H}(\mathrm{NC})$. Compared to this situation, each prosumer's profit must not be less in the grand coalition with the cooperative mode (with DR), which is expressed in (37).

In addition to the subsets $(\{1\},\{2\},\{3\},\ldots,\{n\})$, it is possible that part of the prosumers forms a coalition. In this paper, only one coalition is considered, as there is one manager in the community. Then we have to analyze the prosumers' profits in partial coalition with that in the grand coalition. For any partial coalition $\mathcal{Z} \subseteq \mathcal{N}$, all the prosumers in $\mathcal{Z}$ operate under the

This article has been accepted for publication in a future issue of this journal, but has not been fully edited. Content may change prior to final publication. Citation information: DOI 10.1109/TPWRS.2018.2877236, IEEE Transactions on Power Systems

the cooperative mode (with DR) while the other prosumers in $\mathcal{N}/\mathcal{Z}$ still act in the non-cooperative mode (with DR). Denoting the partial coalition $\mathcal{Z}$ as a whole prosumer z, the profit of the prosumer z in the cooperative mode (with DR) can be represented as follows:

$$-C_z^{t\sim H}(\mathrm{CO}) = -C_z^{t\sim H}(\mathrm{NC}) + \rho_z \cdot \left(E_{\mathrm{add\_}z}^{t\sim H}\right) \tag{39}$$

where $C_z^{t\sim H}(\mathrm{NC})$ is the profit of the prosumer z in the non-cooperative mode (with DR), and $E_{\mathrm{add\_}z}^{t\sim H}$ and ρ_z can be calculated using (35) and (36), respectively. It can also be found that prosumer z's profit in the grand coalition is greater than or equal to that in the non-cooperative mode (with DR).

From the above discussion, the profit of each prosumer or partial coalition in the grand coalition is always not less than those in other subsets. Therefore, the allocation in (37) satisfies the condition for the core in (38) and is in the core. So, the profit allocation scheme in a grand coalition with the cooperative mode (with DR) is stable for all the prosumers.

D. Profit Calculation Model of the Hub Manager

The electric profit of HM in the current period and future periods can be expressed respectively as follows:

$$E_{\mathrm{m}}^{t} = \begin{cases} \left(p_{\mathrm{gb}}^{t} + \dfrac{p_{\mathrm{ms}}^{t}\cdot N_{\mathrm{L}}^{t}}{p_{\mathrm{e\_cchp}}^{t} - N_{\mathrm{L}}^{t}}\right)\cdot \max\left(p_{\mathrm{e\_cchp}}^{t} - N_{\mathrm{L}}^{t}, 0\right) \\ + \left(\dfrac{p_{\mathrm{ms}}^{t}\cdot p_{\mathrm{e\_cchp}}^{t}}{N_{\mathrm{L}}^{t} - p_{\mathrm{e\_cchp}}^{t}}\right)\cdot \max\left(N_{\mathrm{L}}^{t} - p_{\mathrm{e\_cchp}}^{t}, 0\right), & N_{\mathrm{L}}^{t} \ge 0 \\ p_{\mathrm{gb}}^{t}\cdot p_{\mathrm{e\_cchp}}^{t}, & N_{\mathrm{L}}^{t} < 0 \end{cases} \tag{40}$$

$$E_{\mathrm{m},\omega_m}^{h} = \begin{cases} \left(p_{\mathrm{gb}}^{h} + \dfrac{p_{\mathrm{ms}}^{h}\cdot N_{\mathrm{L},\omega_m}^{h}}{p_{\mathrm{e\_cchp}}^{h} - N_{\mathrm{L},\omega_m}^{h}}\right)\cdot \max\left(p_{\mathrm{e\_cchp}}^{h} - N_{\mathrm{L},\omega_m}^{h}, 0\right) \\ + \left(\dfrac{p_{\mathrm{ms}}^{h}\cdot p_{\mathrm{e\_cchp}}^{h}}{N_{\mathrm{L},\omega_m}^{h} - p_{\mathrm{e\_cchp}}^{h}}\right)\cdot \max\left(N_{\mathrm{L},\omega_m}^{h} - p_{\mathrm{e\_cchp}}^{h}, 0\right), & N_{\mathrm{L},\omega_m}^{h} \ge 0 \\ p_{\mathrm{gb}}^{h}\cdot p_{\mathrm{e\_cchp}}^{h} + F_{\mathrm{tm}}^{h}, & N_{\mathrm{L},\omega_m}^{h} < 0 \end{cases} \tag{41}$$

Thus, the total profit of the HM can be represented as:

$$E_{\mathrm{m}}^{t\sim H}(\mathrm{CO}) = E_{\mathrm{m}}^{t} + \sum_{h=t+1}^{H}\sum_{\omega_m\in\Omega}\pi(\omega_m)\cdot E_{\mathrm{m},\omega_m}^{h} - \sum_{h=t}^{H} C_{\mathrm{cchp}}^{h} + F_{\mathrm{tm}}^{t\sim H} \tag{42}$$

The comparison indicates that the HM's profit in the cooperative mode (with DR) is always not smaller than the CCHP manager's profit in the non-cooperative mode (with DR).

E. Each Prosumer's Shiftable Load Determination based on the Contribution Weights

Based on the real-time rolling horizon energy management optimization model in the cooperative trading mode, the total shiftable load of all the prosumers is determined. However, in practical applications, the shiftable load of each prosumer also needs to be derived. After obtaining the optimized total shiftable load, the shiftable load of each prosumer should meet the following constraints:

$$\begin{aligned} \textbf{s.t.}\quad & l_{si}^{h\_\min} < l_{si}^{h} < l_{si}^{h\_\max}, h \in [\alpha_i, \beta_i] \\ & l_{si}^{h} = 0, \quad h \notin [\alpha_i, \beta_i] \\ & \sum_{h=t}^{H} l_{si}^{h} = Q_i - \sum_{h=1}^{t-1} l_{si\_\mathrm{opt}}^{h} \\ & \sum_{i=1}^{n} l_{si}^{h} = l_{\mathrm{s\_opt}}^{h}, \quad h \in [t, H] \end{aligned} \tag{43}$$

There are many possible schemes for shifting prosumers' loads which meet the expression (43). In this paper, it is assumed that the prosumer with a larger contribution should have a higher priority in ensuring its comfort level, which is reflected by the gap between the original shiftable loads and the optimized shiftable loads. Based on this principle, an optimization objective function is proposed as follows:

$$\min \quad \sum_{t}^{H}\sum_{i=1}^{n}\rho_i\cdot\left[l_{si}^{h} - l_{si}^{h}(0)\right]^2 \tag{44}$$

where $l_{si}^{h}(0)$ is the original shiftable load of prosumer i in period h, i.e., the value before the demand response optimization is performed.

After the optimization model consisting of (43) and (44) is solved by the HM, the shiftable load of each prosumer can be obtained.

V. Equivalent Method and Implementation Process for the Optimization Model

According to the above discussions, the optimization objective under the cooperative mode (with DR) (expression (23)) and each prosumer's optimization objective under the non-cooperative mode (with DR) (expression (59)) are both segmented functions. The nonlinear programming models with segmented objective functions can't be solved directly by nonlinear programming software. In this paper, we transform these nonlinear programming models into MILP models by adding several auxiliary variables [27], so that the converted models can be solved directly using some existing optimization solvers. Taking the cooperative mode (with DR) as an example, its equivalent model mainly focuses on the first two terms in (23), i.e., the current period cost and the future period costs.

A. Equivalent Expression of Current Period Cost

For the current-period cost, there are 3 segmentation points, a (the minimum value of the variable l_{s}^{t}), b (the maximum value of the variable l_{s}^{t}), and $P^t - l_{\mathrm{f}}^{t}$ (where the current period cost is zero). Based on auxiliary variables φ_1^t, φ_2^t, φ_3^t, z_1^t and z_2^t, l_{s}^{t} and current period cost C^t can be expressed as:

$$l_{\mathrm{s}}^{t} = \varphi_1^t\cdot a + \varphi_2^t\cdot\left(P^t - l_{\mathrm{f}}^{t}\right) + \varphi_3^t\cdot b \tag{45}$$

$$C^t = \varphi_1^t\cdot C^t(a) + \varphi_2^t\cdot C^t\left(P^t - l_{\mathrm{f}}^{t}\right) + \varphi_3^t\cdot C^t(b) \tag{46}$$

B. Equivalent Expression of Future-Period Cost

For the future-period cost, there are 2+M segmentation points, a (the minimum value of the variable l_{s}^{h}), b (the maximum value of the variable l_{s}^{h}), and other M segment points: $l_{\mathrm{s}}^{h} = P_{\omega_m}^{h} - l_{\mathrm{f},\omega_m}^{h}, \omega_m \in \Omega$. We rearrange these M segmentation points from the smallest to the largest, and the corresponding scenario set can be expressed as $\Omega^h = \left[\omega_1^h, \ldots, \omega_{m'}^h, \ldots, \omega_M^h\right]$. This means in each future period, the scenario sequence could be adjusted. We define an ordering function R_h to express the relationship between m' (scenario subscript in Ω^h) and m (scenario subscript in Ω):

$$m' = R_h(m) \tag{47}$$

In period h, the rearranged segment points can be represented as $\left[a, P_1^h - l_{\mathrm{f},1}^h, \ldots, P_k^h - l_{\mathrm{f},k}^h, \ldots, P_M^h - l_{\mathrm{f},M}^h, b\right]$. Adding auxiliary variables $\left[\varphi_1^h, \ldots, \varphi_{M+2}^h\right]$ and $\left[z_1^h, \ldots, z_{M+1}^h\right]$, l_{s}^{h} and C^h can be expressed as:

This article has been accepted for publication in a future issue of this journal, but has not been fully edited. Content may change prior to final publication. Citation information: DOI 10.1109/TPWRS.2018.2877236, IEEE Transactions on Power Systems

$$l_{\mathrm{s}}^{h}=\varphi_{1}^{h}\cdot a+\sum_{k=1}^{M}\varphi_{k+1}^{h}\cdot\left(P_{k}^{h}-l_{\mathrm{f},k}^{h}\right)+\varphi_{M+2}^{h}\cdot b \tag{48}$$

$$C^{h}=\varphi_{1}^{h}\cdot C^{h}\left(a\right)+\sum_{k=1}^{M}\varphi_{k+1}^{h}\cdot C^{h}\left(P_{k}^{h}-l_{\mathrm{f},k}^{h}\right)+\varphi_{M+2}^{h}\cdot C^{h}\left(b\right) \tag{49}$$

where,

$$C^{h}\left(a\right)=\sum_{m'=1}^{M}\pi\left(\omega_{m'}\right)\cdot p_{\mathrm{mb}}^{h}\cdot\left(l_{\mathrm{f},\omega_{m'}}^{h}+a-P_{\omega_{m'}}^{h}\right) \tag{50}$$

$$\begin{aligned}C^{h}\left(P_{k}^{h}-l_{\mathrm{f},k}^{h}\right)=&\sum_{m'=1}^{k-1}\pi\left(\omega_{m'}\right)\cdot p_{\mathrm{ms}}^{h}\cdot\left[l_{\mathrm{f},\omega_{m'}}^{h}+\left(P_{k}^{h}-l_{\mathrm{f},k}^{h}\right)-P_{\omega_{m'}}^{h}\right]+\\&\sum_{m'=k+1}^{M}\pi\left(\omega_{m'}\right)\cdot p_{\mathrm{mb}}^{h}\cdot\left[l_{\mathrm{f},\omega_{m'}}^{h}+\left(P_{k}^{h}-l_{\mathrm{f},k}^{h}\right)-P_{\omega_{m'}}^{h}\right],\\&k\in\left[1,2,\cdots,M\right]\end{aligned} \tag{51}$$

$$C^{h}\left(b\right)=\sum_{m'=1}^{M}\pi\left(\omega_{m'}\right)\cdot p_{\mathrm{ms}}^{h}\cdot\left(l_{\mathrm{f},\omega_{m'}}^{h}+b-P_{\omega_{m'}}^{h}\right) \tag{52}$$

C. Equivalent Expression of Overall Energy Management Optimization Model

According to the previous section, the model of the cooperative mode (with DR) can be expressed as follows.

1) The objective function of the equivalent model

$$\begin{aligned}\textbf{min}\ C^{t\sim H}=&\varphi_{1}^{t}\cdot C^{t}\left(a\right)+\varphi_{2}^{t}\cdot C^{t}\left(P^{t}-l_{\mathrm{f}}^{t}\right)+\varphi_{3}^{t}\cdot C^{t}\left(b\right)\\&+\sum_{h=t+1}^{H}\left[\varphi_{1}^{h}\cdot C^{h}\left(a\right)+\sum_{k=1}^{M}\varphi_{k+1}^{h}\cdot C^{h}\left(P_{k}^{h}-l_{\mathrm{f},k}^{h}\right)+\varphi_{M+2}^{h}\cdot C^{h}\left(b\right)\right]\\&+\gamma\cdot\left[\alpha+\frac{1}{1-\beta}\cdot\sum_{\omega_{m}\in\Omega}\pi\left(\omega_{m}\right)\cdot u\left(\omega_{m}\right)\right]+F_{\mathrm{tm}}^{t\sim H}\end{aligned} \tag{53}$$

2) Constraints of the equivalent model

$$\begin{aligned}\textbf{s.t.1}\ \ &l_{\mathrm{s}}^{t\_\min}<\varphi_{1}^{t}\cdot a+\varphi_{2}^{t}\cdot\left(P^{t}-l_{\mathrm{f}}^{t}\right)+\varphi_{3}^{t}\cdot b<l_{\mathrm{s}}^{t\_\max},t\in\left(\bigcup_{i=1}^{n}[\alpha_{i},\beta_{i}]\right)\\&\varphi_{1}^{t}\cdot a+\varphi_{2}^{t}\cdot\left(P^{t}-l_{\mathrm{f}}^{t}\right)+\varphi_{3}^{t}\cdot b=0\qquad,t\notin\left(\bigcup_{i=1}^{n}[\alpha_{i},\beta_{i}]\right)\\&z_{1}^{t}+z_{2}^{t}=1,\quad z_{1}^{t},z_{2}^{t}=0,1\\&\varphi_{1}^{t}+\varphi_{2}^{t}+\varphi_{3}^{t}=1,\quad\varphi_{1}^{t},\varphi_{2}^{t},\varphi_{3}^{t}\geq0\\&\varphi_{1}^{t}\leq z_{1}^{t},\quad\varphi_{2}^{t}\leq z_{1}^{t}+z_{2}^{t},\quad\varphi_{3}^{t}\leq z_{2}^{t}\end{aligned} \tag{54}$$

$$\begin{aligned}\textbf{s.t.2}\ \ &l_{\mathrm{s}}^{h\_\min}<\varphi_{1}^{h}\cdot a+\sum_{k=1}^{M}\varphi_{k+1}^{h}\cdot\left(P_{k}^{h}-l_{\mathrm{f},k}^{h}\right)+\varphi_{M+2}^{h}\cdot b<l_{\mathrm{s}}^{h\_\max},h\in\left(\bigcup_{i=1}^{n}[\alpha_{i},\beta_{i}]\right)\\&\varphi_{1}^{h}\cdot a+\sum_{k=1}^{M}\varphi_{k+1}^{h}\cdot\left(P_{k}^{h}-l_{\mathrm{f},k}^{h}\right)+\varphi_{M+2}^{h}\cdot b=0\qquad,h\notin\left(\bigcup_{i=1}^{n}[\alpha_{i},\beta_{i}]\right)\\&\sum_{k=1}^{M+1}z_{k}^{h}=1,\quad z_{1}^{h},z_{2}^{h},\cdots,z_{M+1}^{h}=0,1\\&\sum_{k=1}^{M+2}\varphi_{k}^{h}=1,\quad\varphi_{1}^{h},\varphi_{2}^{h},\cdots,\varphi_{M+2}^{h}\geq0\\&\varphi_{1}^{h}\leq z_{1}^{h},\cdots,\varphi_{j}^{h}\leq z_{j-1}^{h}+z_{j}^{h},\cdots,\varphi_{M+2}^{h}\leq z_{M+1}^{h},\ j=2,3,\cdots,M+1\end{aligned} \tag{55}$$

$$\begin{aligned}\textbf{s.t.3}\quad&u\left(\omega_{m}\right)\geq0\\&-\sum_{h=t+1}^{H}C_{\omega_{R_{h}(m)}^{h}}^{h}+\alpha+u\left(\omega_{m}\right)\geq0\end{aligned} \tag{56}$$

where $C_{\omega_{R_h(m)}^{h}}^{h}$ can be calculated using the following expression:

$$\begin{aligned}C_{\omega_{R_{h}(m)}^{h}}^{h}=&p_{\mathrm{mb}}^{h}\cdot\left(l_{\mathrm{f},\omega_{R_{h}(m)}^{h}}^{h}+a-P_{\omega_{R_{h}(m)}^{h}}^{h}\right)\cdot\varphi_{1}^{h}\\&+\sum_{k=1}^{R_{h}(m)-1}\left\{p_{\mathrm{mb}}^{h}\cdot\left(l_{\mathrm{f},\omega_{R_{h}(m)}^{h}}^{h}+\left[P_{k}^{h}-l_{k}^{h}\right]-P_{\omega_{R_{h}(m)}^{h}}^{h}\right)\cdot\varphi_{k+1}^{h}\right\}\\&+\sum_{k=1}^{R_{h}(m)+1}\left\{p_{\mathrm{ms}}^{h}\cdot\left(l_{\mathrm{f},\omega_{R_{h}(m)}^{h}}^{h}+\left[P_{k}^{h}-l_{k}^{h}\right]-P_{\omega_{R_{h}(m)}^{h}}^{h}\right)\cdot\varphi_{k+1}^{h}\right\}\\&+p_{\mathrm{ms}}^{h}\cdot\left(l_{\mathrm{f},\omega_{R_{h}(m)}^{h}}^{h}+b-P_{\omega_{R_{h}(m)}^{h}}^{h}\right)\cdot\varphi_{M+2}^{h}\end{aligned} \tag{57}$$

D. The Implementation Process of Energy Management

The implementation process of the cooperative trading mode is shown in Fig. 4. The left part in the process is performed by UEMS of each prosumer, while the right part is performed by the HM. The information exchanged automatically between the HM and prosumers is also indicated in Fig. 4. The flowchart in the dashed box indicates the implementation process of the non-cooperative mode (with DR).

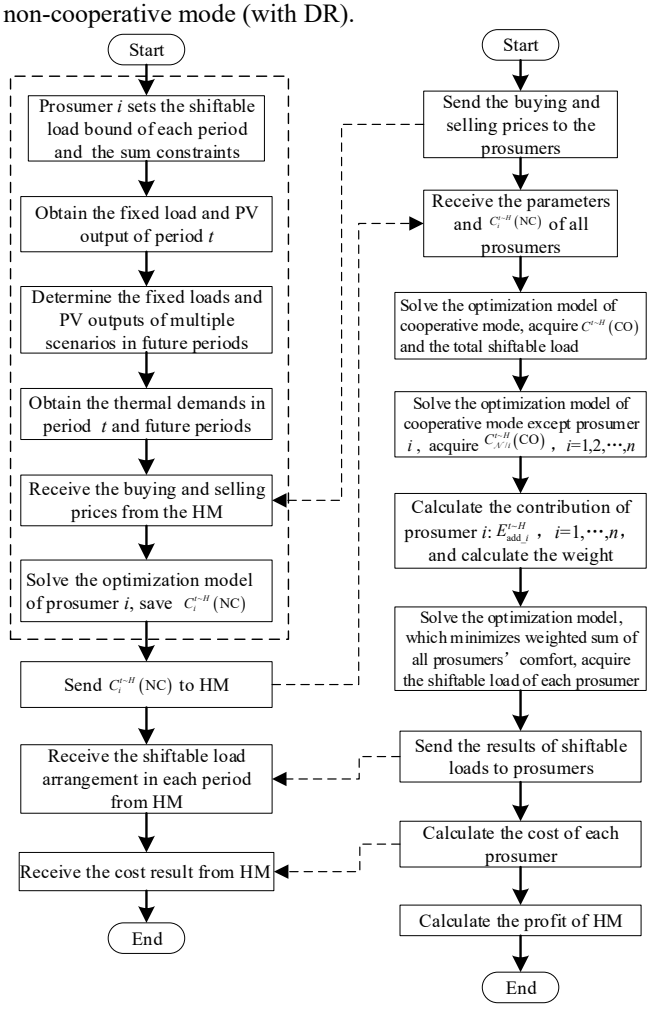

Fig. 4. The flowchart of proposed cooperative trading mode.

VI. Case Studies

A. Basic Data

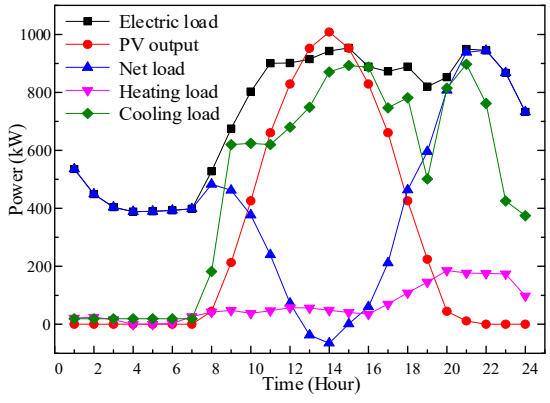

Fig. 5. Total power curves of all prosumers in a typical day

The proposed model is applied in a CES, and the MATLAB

This article has been accepted for publication in a future issue of this journal, but has not been fully edited. Content may change prior to final publication. Citation information: DOI 10.1109/TPWRS.2018.2877236, IEEE Transactions on Power Systems

software package is employed to solve the optimization problems using the data from smart meters. The community consists of two office buildings (OB) and four residential buildings (RB), and they are all treated as prosumers with roof-top PV panels. All of the prosumers possess PV systems with the capacity of 160 or 200 kWp. The load and PV power for a typical summer day are shown in Fig. 5.

In this case, the proportion of shiftable loads' electricity is close to 30%. We denote $\boldsymbol{p}_{\mathrm{gs}}$ to be peak valley electricity prices, and set each element of $\boldsymbol{p}_{\mathrm{bs}}$ to be the same value of 0.48 Yuan/kWh. The other relevant parameters in this case are shown in Table I.

TABLE I THE RELATED PARAMETERS

Name of parameter	Value of parameter	Name of parameter	Value of parameter
η_{chp}	0.4	r_c	0.12 Yuan/kWh
η_{loss}	0.05	r_h	0.15 Yuan/kWh
δ_{heat}	0.8	γ	0.2
δ_{cool}	1.2	β	0.8
p_{gas}	1.5 Yuan/m^3	m	10

B. Results of Multi-scenario Determination

The optimization models in this paper consider the cost in the future, so they depend on the predicted quantities of certain variables. As there usually exist errors in the forecasting outcomes, we utilize a multi-scenario determination method based on the probability distribution of variables' prediction error to deal with the stochastic optimization problems (the multi-scenario determination models are introduced in **Appendix B**). Two stochastic variables are considered in this paper, i.e., the PV output and the fixed load. Firstly, the scenarios of each variable need to be determined. Taking the point with the highest probability density as the center, 12 error points are sampled to the left and the right sides respectively in the step length of 3% (the parameters of the distribution function are estimated based on [28]). Then there are 15 scenarios for each variable, and as a result, there are 225 scenarios considering both variables. To reduce the calculation burden, the number of scenarios is reduced to 10 using the K-means clustering method [29]. The calculated results of these 10 scenarios are shown in Table II.

TABLE II THE MULTI-SCENARIO RESULTS

Name of the scenario	Prediction error of PV output	Prediction error of fixed load	Probability of the scenario
ω_1	-15.38%	14.70%	0.01
ω_2	13.34%	2.29%	0.13
ω_3	-7.38%	-12.50%	0.02
ω_4	9.84%	13.09%	0.08
ω_5	4.36%	-12.51%	0.04
ω_6	-12.50%	-3.45%	0.03
ω_7	1.56%	-0.81%	0.41
ω_8	14.98%	-8.73%	0.03
ω_9	-7.55%	4.84%	0.11
ω_{10}	-0.92%	13.14%	0.13

C. Comparison of Cooperative Mode (with DR) and Non-Cooperative Mode (with DR)

Setting the current period as 1:00 a.m. in the typical day, we solve the optimization models with the two trading modes based on the multi-scenario results (the implementation process is described in **Section V-D**). The MILP models have been solved using Gurobi optimizer under Matlab using an Intel Core-i5 2.2-GHz personal computer. It took 3.29 seconds to realize the whole implementation process.

1) The shiftable loads and system net loads

The total shiftable loads and net loads of different building types with the two optimization models are shown in Fig. 6. The backgrounds in figures of the shiftable loads were colored according to the electricity selling prices. The non-cooperative mode (without DR) means that the prosumers operate under the non-cooperative trading mode, but they do not perform any demand response optimization.

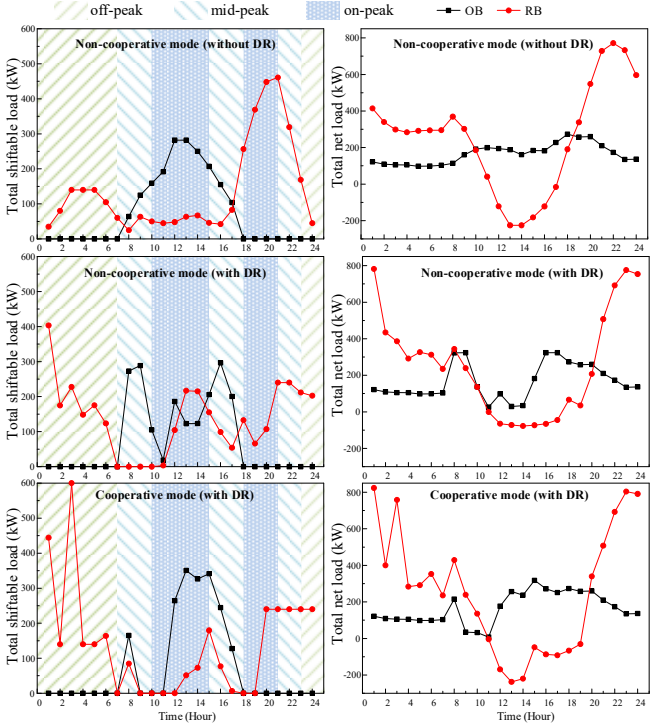

Fig. 6. Curves of total shiftable loads and net loads of different building types. The off-peak, mid-peak, and on-peak prices are set to be 0.50, 0.84, and 1.32 Yuan/kWh, respectively.

According to Fig. 6, under the non-cooperative mode (without DR), it can be observed that the OBs' shiftable loads are mainly used in the daytime, while the RBs' shiftable loads are distributed more dispersedly with an apparent load peak during the night.

Compared with the non-cooperative mode (without DR), the shiftable loads have been moved to the low price periods under the non-cooperative mode (with DR). For OBs, two load peaks appear in periods 8:00~9:00 a.m. and 3:00~5:00 p.m.with the lowest prices in the daytime. For RBs, a great part of shiftable loads have been moved to the period 1:00~6:00 a.m. with the lowest price all the day. As RBs' PV systems generate the most redundant power outputs during 1:00~3:00 p.m., a small peak also appears in that period.

Comparing the results of cooperative mode (with DR) with those of non-cooperative mode (with DR), the OBs' shiftable loads have been significantly increased during 1:00~3:00 p.m.

This article has been accepted for publication in a future issue of this journal, but has not been fully edited. Content may change prior to final publication. Citation information: DOI 10.1109/TPWRS.2018.2877236, IEEE Transactions on Power Systems

(with the highest prices), while the RB's shiftable loads have been reduced in this period although PV outputs are sufficient. All these changes imply that the RBs can share more PV power to OBs, and cut the total cost of prosumers' grand coalition.

The obtained results of system net loads are shown in Fig. 7. According to Fig. 7, the optimized peaks of the system net loads in these two optimization models are almost the same as that in the non-cooperative mode (without DR). For the valleys of the system net loads around 1:00~2:00 p.m., the value under cooperative mode (with DR) is close to zero, which means that the prosumers do not need to sell the PV power back to the grid. However, the system net loads around the same periods with the non-cooperative mode (with DR) is lower by almost 100 kW. In addition, the maximum net loads of both optimization models are less than or equal to that of the non-cooperative mode (without DR), which means the proposed optimization models have not brought more peak shaving burden to the utility grid.

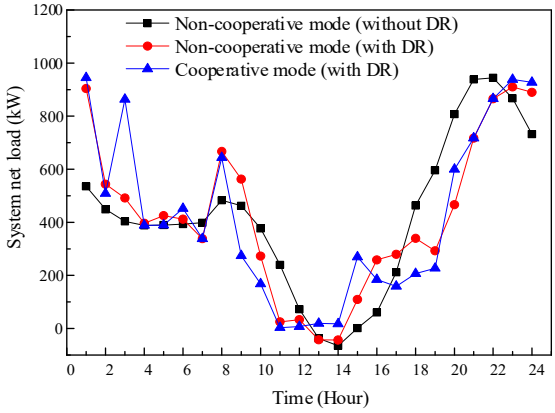

Fig. 7. Curves of the system net load with two optimization models.

2) The prosumers' costs and HM's profits

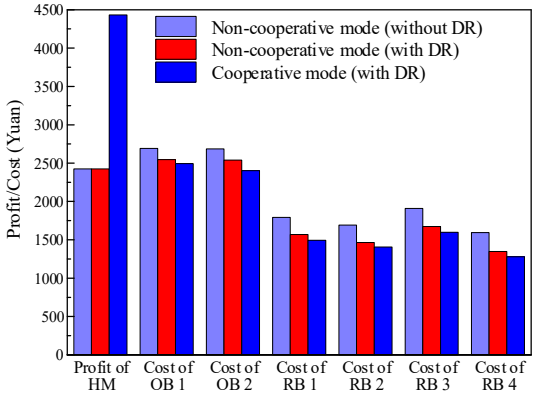

Fig. 8. The HM's profits and the prosumers' costs.

In this section, we compare the prosumers' costs and HM's profits with different trading modes. As seen from Fig. 8, the CCHP manager's profit in the non-cooperative mode (with DR) is the same as that in the non-cooperative mode (without DR), as the electric outputs of the CCHP system are all purchased by the utility grid in these two modes. However, in the cooperative trading mode (with DR), the HM's profit has been significantly enhanced by 83% compared to the CCHP manager's profit. This is mainly because the produced electricity of the CCHP system is sold to the prosumers first with more competitive prices in the cooperative trading mode, compared with the buying prices of utility grid in non-cooperative trading modes.

For prosumers, costs of the non-cooperative mode (with DR) are reduced by 10% compared to the non-cooperative mode (without DR); costs of the cooperative mode (with DR) have been reduced by 4% compared to the non-cooperative mode (with DR), and by 14% compared to the non-cooperative mode (without DR). Subentry values of prosumers' total cost and HM's profit in cooperative trading mode (with DR) are listed in Table III.

TABLE III THE COMPONENTS OF PROSUMERS' TOTAL COST AND HM'S PROFIT UNDER COOPERATIVE MODE (WITH DR)

Components of prosumers' total cost	Result (Yuan)	Components of HM' s profit	Result (Yuan)
Total electrical cost	7396	Total electrical profit	6081
CVaR value	1647	CCHP's cost	3283
Thermal cost	1633	Thermal profit	1633

D. Sensitivity Analysis of HM's Prices and CVaR parameters

1) Sensitivity analysis of HM's selling prices

In the previous section, the selling prices of HM are set to be the same as the utility grid. In reality, the HM is able to adjust its selling prices (as it possesses the generating equipment) to attract prosumers to join the coalition with lower selling prices. It is assumed that HM decreases the selling prices with a coefficient c_{cut}, and the adjusted selling price can be expressed as follows:

$$p_{\text{ms}}^{h} = p_{\text{gs}}^{h} - c_{\text{cut}} \cdot \left(p_{\text{gs}}^{h} - p_{\text{gb}}^{h} \right) \tag{58}$$

The prosumers' cost saving ratio and HM's profit increase ratio as a function of c_{cut} are shown in Fig. 9. The ratios here represent the value variation between the cooperative mode (with DR) with the non-cooperative mode (with DR).

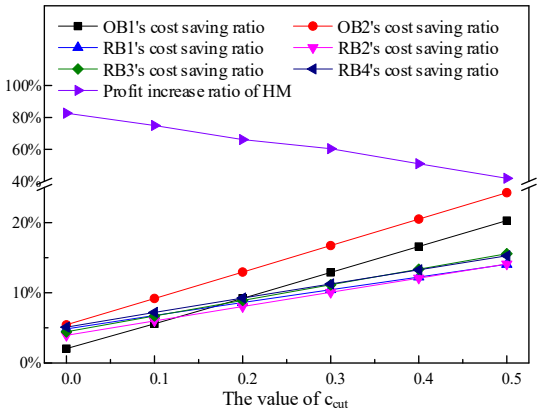

Fig. 9. The prosumers' cost saving ratio and HM's profit increase ratio with different c_{cut}.

According to Fig. 9, the HM's profit increase ratio will decrease from 83% to 42% when c_{cut} changes from 0.0 to 0.5. Meanwhile, the cost saving ratios have increased differently for each prosumer. The total prosumers' cost saving ratio has increased from 4% to 18%. The sensitivity analysis of c_{cut} means that the profit of HM has been transferred to the prosumers when HM decreases its selling prices.

2) Sensitivity analysis of parameter γ

The prosumers' cost saving ratio and HM's profit increase ratio as a function of γ are shown in Fig.10.

It is observed that the HM's profit increase ratio and the OBs'

This article has been accepted for publication in a future issue of this journal, but has not been fully edited. Content may change prior to final publication. Citation information: DOI 10.1109/TPWRS.2018.2877236, IEEE Transactions on Power Systems

cost saving ratios do not depend on γ, while the RBs' cost saving ratios decrease when γ increases. The possible reason why γ has a more noticeable effect on OBs' cost saving ratios is that only the OBs possess shareable PV output according to the top right subplot in Fig. 6, and the uncertainty of the PV output will influence the CVaR value more obviously, so the larger γ means the more CVaR cost for the OBs.

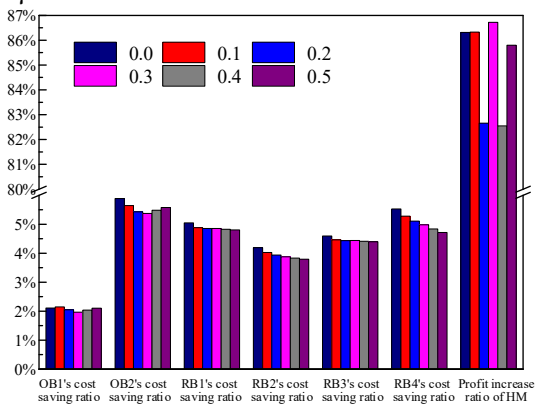

Fig. 10. The prosumers' cost saving ratio and HM's profit increase ratio with different γ.

VII. Conclusion

In this paper, we proposed a cooperative trading mode for the CES consisting CEH and PV prosumers firstly. A corresponding real-time rolling horizon energy management model for the CES was studied from a cooperative perspective. The cooperation is mainly embodied in two aspects: the cooperation between HM and the prosumer cluster; and the cooperation among all the prosumers in the community. We also proposed a new model based on the non-cooperative trading mode which is used as a benchmark. These two models both consider the stochastic characteristics of some parameters in the real-time rolling horizon energy management process. We established the optimization models considering the cost of all time and the CVaR values. The optimization models are transformed into MILP ones by adding multiple auxiliary variables. The case studies have shown that the cooperative model can promote local consumption of PV energy, increase the profit of the manager, and reduce the costs of prosumers in the community significantly compared with the non-cooperative models. The effect of the proposed cooperative model in a specific application is relevant to the net loads' characteristics of the prosumers. Stronger complementarity of prosumers' net loads results in a greater value of the proposed model.

APPENDIX A
Non-cooperative Trading Mode & Optimization Model

A.1 The Framework of Non-cooperative Trading Mode

In this section, the non-cooperative trading mode is introduced, which is used as a benchmark for the cooperative trading mode. The schematic diagram of the non-cooperative trading mode is shown in Fig. 11.

According to Fig. 11, in the non-cooperative mode, the CCHP is in charge of providing thermal output to all the prosumers in the community. The electricity generated simultaneously is purchased by the utility grid based on its buying prices.

For each prosumer in the community, PV source is the first choice of electric power, and he/she will purchase electricity from the utility grid with its selling prices when PV source cannot satisfy the load demands. On the other hand, if the demand of the prosumer is less than the production of PV source, the surplus PV power will be sold to the utility grid.

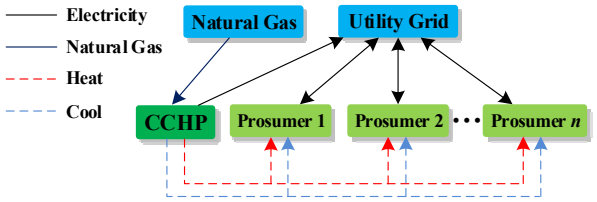

Fig. 11. Schematic diagram of the non-cooperative trading mode.

A.2 The Real-time Rolling Horizon Energy Management Optimization Model in the Non-cooperative Trading Mode

In the non-cooperative trading mode, the real-time rolling horizon energy management optimization is conducted by the UEMS of each prosumer in the community. So, the optimization model in the non-cooperative mode can be regarded as an independent optimization model. The optimization model consists of two parts, i.e., the objective function and the constraints.

1) Objective function of the optimization problem

$$\begin{aligned}\textbf{min}\quad C_i^{t\sim H} &= P_{\mathrm{G},i}^t\cdot\left(l_{\mathrm{fi}}^t+l_{\mathrm{si}}^t-P_i^t\right)\\ &+\sum_{\omega_{i,m}\in\Omega_i}\left\{\pi\left(\omega_{i,m}\right)\cdot\sum_{h=t+1}^{H}\left[P_{\mathrm{G},i,\omega_{i,m}}^h\cdot\left(l_{\mathrm{fi},\omega_{i,m}}^h+l_{\mathrm{si}}^h-P_{i,\omega_{i,m}}^h\right)\right]\right\}\\ &+\gamma\cdot\left[\alpha_i+\frac{1}{1-\beta}\cdot\sum_{\omega_{i,m}\in\Omega_i}\pi\left(\omega_{i,m}\right)\cdot u\left(\omega_{i,m}\right)\right]+F_{\mathrm{tmi}}^{t\sim H}\end{aligned} \tag{59}$$

where $C_i^{t\sim H}$ is the overall cost of prosumer i from period t to period H; $P_{\mathrm{G},i}^t$ is the electricity price, which is used in the trading between the prosumers and the utility grid; l_{fi}^t, l_{si}^t, and P_i^t are the fixed load, shiftable load and PV output of the prosumer i at period t (current period) respectively; $\omega_{i,m}$ is the m-th scenario of the prosumer i, Ω_i is the scenario set of the prosumer i, $\pi(\omega_{i,m})$ is the probability of the m-th scenario, $P_{\mathrm{G},i,\omega_{i,m}}^h$ is the trading price of the prosumer i at period h under the m-th scenario, $l_{\mathrm{fi},\omega_{i,m}}^h$, $P_{i,\omega_{i,m}}^h$ are the fixed load and PV output of the prosumer i at period h respectively under the m-th scenario, l_{si}^h is the shiftable load of the prosumer i at period h (future period); γ is the weight of the CVaR value, β is the confidence level, α_i is the value at risk (VaR) of the prosumer i with β, $u(\omega_{i,m})$ is the auxiliary variable under the scenario $\omega_{i,m}$; $F_{\mathrm{tmi}}^{t\sim H}$ is the thermal fee the prosumer i paid to the HM from period t to period H. Ω_i can be defined as:

$$\Omega_i \triangleq \left[\omega_{i,1},\cdots,\omega_{i,M}\right] \tag{60}$$

The prices provided by the utility grid are defined as:

$$\boldsymbol{p}_{\mathrm{gs}} \triangleq [p_{\mathrm{gs}}^1,\ldots,p_{\mathrm{gs}}^H] \tag{61}$$

$$\boldsymbol{p}_{\mathrm{gb}} \triangleq [p_{\mathrm{gb}}^1,\ldots,p_{\mathrm{gb}}^H] \tag{62}$$

where $\boldsymbol{p}_{\mathrm{gs}}$ is the selling price set of the utility grid, and $\boldsymbol{p}_{\mathrm{gb}}$

This article has been accepted for publication in a future issue of this journal, but has not been fully edited. Content may change prior to final publication. Citation information: DOI 10.1109/TPWRS.2018.2877236, IEEE Transactions on Power Systems

is the buying price set. The relationship between the utility grid's prices and $P_{\mathrm{G},i}^{t}$ or $P_{\mathrm{G},i,\omega_{i,m}}^{h}$ can be defined as:

$$P_{\mathrm{G},i}^{\mathrm{t}}=\begin{cases}p_{\mathrm{gs}}^{\mathrm{t}} & ,l_{\mathrm{fi}}^{t}+l_{si}^{t}-P_{i}^{t}\geq 0\\ p_{\mathrm{gb}}^{\mathrm{t}} & ,l_{\mathrm{fi}}^{t}+l_{si}^{t}-P_{i}^{t}<0\end{cases} \tag{63}$$

$$P_{\mathrm{G},i,\omega_{i,m}}^{h}=\begin{cases}p_{\mathrm{gs}}^{h} & ,l_{\mathrm{fi},\omega_{i,m}}^{h}+l_{si}^{h}-P_{i,\omega_{i,m}}^{h}\geq 0\\ p_{\mathrm{gb}}^{h} & ,l_{\mathrm{fi},\omega_{i,m}}^{h}+l_{si}^{h}-P_{i,\omega_{i,m}}^{h}<0\end{cases} \tag{64}$$

As the prices in the objective are segmented functions, the optimization model is in fact a nonlinear programming model. The optimized result can be defined as $C_{i}^{t\sim H}(\mathrm{NC})$, i.e., the optimum overall cost of the prosumer *i* in the non-cooperative trading mode.

2) Constraints of the optimization problem

The constraints fall into two categories. The first one is the constraints relating to the shiftable loads, which are shown in (65). The second one is related to the CVaR [24], which is shown in (66).

$$\begin{aligned}\textbf{s.t.}1\quad & l_{si}^{h\_\min}<l_{si}^{h}<l_{si}^{h\_\max},h\in[\alpha_i,\beta_i]\\ & l_{si}^{h}=0\qquad\quad ,h\notin[\alpha_i,\beta_i]\\ & \textstyle\sum_{h=t}^{H}l_{si}^{h}=Q_i-\sum_{h=1}^{t-1}l_{si\_\mathrm{opt}}^{h}\end{aligned} \tag{65}$$

$$\begin{aligned}\textbf{s.t.}2\quad & u(\omega_{i,m})\geq 0\\ & -\sum_{h=t+1}^{H}\left[P_{\mathrm{G},i,\omega_{i,m}}^{h}\cdot\left(l_{\mathrm{fi},\omega_{i,m}}^{h}+l_{si}^{h}-P_{i,\omega_{i,m}}^{h}\right)\right]+\alpha_i+u(\omega_{i,m})\geq 0\end{aligned} \tag{66}$$

A.3 Profit Calculation Model of CCHP Manager

According to the framework of the non-cooperative trading mode, the profit of the manager can be expressed as:

$$E_{\mathrm{m}}^{t\sim H}(NC)=\sum_{h=t}^{H}\left(p_{\mathrm{gb}}^{h}\cdot p_{\mathrm{e\_cchp}}^{h}-C_{\mathrm{cchp}}^{h}+\textstyle\sum_{i=1}^{n}F_{\mathrm{tmi}}^{h}\right) \tag{67}$$

In the energy management model, the manager does not take part in the optimization process, who only needs to calculate its profit based on the optimized results of prosumers.

APPENDIX B
THE MULTI-SCENARIO DETERMINATION MODELS

The prediction error conforms to the hyperbolic distribution characteristics [28], which is shown in Fig. 12.

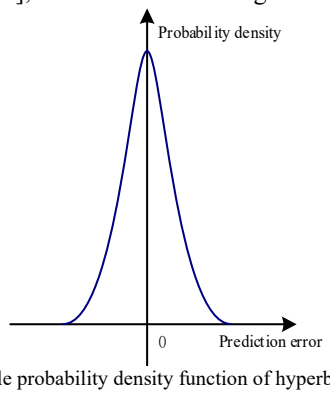

Fig. 12. An example probability density function of hyperbolic distribution.

The probability density function of the hyperbolic distribution can be represented as:

$$f(x)=\frac{1}{2\cdot\sqrt{1+\pi^2}\cdot K_1(\zeta)}\cdot\mathrm{e}^{\left\{-\zeta\cdot\left[\sqrt{1+\pi^2}\cdot\sqrt{1+\left(\frac{x-\mu}{\delta}\right)^2}-\pi\cdot\frac{x-\mu}{\delta}\right]\right\}} \tag{68}$$

where $K_\lambda(\zeta)$ is defined as:

$$K_\lambda(\zeta)=\frac{1}{2}\int_0^\infty \zeta^{\lambda-1}\cdot\mathrm{e}^{\left(-\zeta\cdot\frac{\left(\mathrm{x}+\frac{1}{\mathrm{x}}\right)}{2}\right)}\mathrm{dx} \tag{69}$$

1) Scenario determination method of a single stochastic variable

We adopt the equal step length sampling method to determine the scenarios of a single stochastic variable. Taking the error point $\mathrm{x}_{r(0)}$ which corresponds to the highest probability density $f_r(\mathrm{x}_{r(0)})$ as the center, we sample N_r error points to the left and right sides respectively in an equal step length. The sampling points can be denoted as $\mathrm{x}_{r(1)}$, $\mathrm{x}_{r(-1)}$, $\mathrm{x}_{r(2)}$, $\mathrm{x}_{r(-2)}$ …… $\mathrm{x}_{r(N_r)}$, $\mathrm{x}_{r(-N_r)}$, and their corresponding probabilities are $f_r(\mathrm{x}_{r(1)})$, $f_r(\mathrm{x}_{r(-1)})$, $f_r(\mathrm{x}_{r(2)})$, $f_r(\mathrm{x}_{r(-2)})$ …… $f_r(\mathrm{x}_{r(N_r)})$, $f_r(\mathrm{x}_{r(-N_r)})$. For each single stochastic variable, this method can be used to determine its sampling points and corresponding probabilities.

2) Scenario determination method of multiple stochastic variables

Based on the scenarios of a single stochastic variable in step 1), the scenarios of multiple stochastic variables can be obtained by combinations. In every scenario of multiple stochastic variables, it consists of scenarios from every single stochastic variable, so there are $N_{\text{multi-scenario}}=\prod_{r=1}^{R}(2*N_r+1)$ scenarios when *R* stochastic variables exist. The *k*-th scenario of multiple stochastic variables can be denoted as:

$$\left[x_{1(k_1)},x_{2(k_2)},\cdots,x_{R(k_R)}\right],\ k_r\in[0,1,-1,\cdots,N_r,-N_r],r\in[1,\cdots,R] \tag{70}$$

The probability of this scenario can be calculated based on the scenario probability of each single stochastic variable:

$$f\left[x_{1(k_1)},x_{2(k_2)},\cdots,x_{R(k_R)}\right]=\prod_{r=1}^{R}f_r\left(x_{r(k_r)}\right) \tag{71}$$

After obtaining the probabilities of all scenarios, normalization is performed and the ultimate probability of the *k*-th scenario is:

$$f'\left[x_{1(k_1)},x_{2(k_2)},\cdots,x_{R(k_R)}\right]=\frac{\prod_{r=1}^{R}f_r\left(x_{r(k_r)}\right)}{\sum_{k=1}^{N_{\text{multi-scenario}}}\left[\prod_{r=1}^{R}f_r\left(x_{r(k_r)}\right)\right]} \tag{72}$$

3) Scenarios reduction based on K-means method

As there are $\prod_{r=1}^{R}(2*N_r+1)$ scenarios with *R* stochastic variables, too many scenarios will increase the complexity and calculation time of the optimization model. We adopt the K-means method to reduce the number of scenarios [29]. If assuming there will be *M* scenarios in the energy management model, then the number of clustering centers is *M*. The set of samples in the *m*-th category can be denoted as Ω_m, which consists of N_m samples. The clustering center of the *m*-th category corresponds to scenario ω_m, and the value of each stochastic variable is calculated by:

$$\boldsymbol{x}_{c\_\Omega_m}=\frac{\sum_{\left[x_{1(k_1)},x_{2(k_2)},\cdots,x_{R(k_R)}\right]\in\Omega_m}\left[x_{1(k_1)},x_{2(k_2)},\cdots,x_{R(k_R)}\right]}{N_m} \tag{73}$$

The probability of scenario ω_m is the sum of all the scenarios' probabilities in Ω_m:

$$\pi(\omega_m)=\sum_{\left[x_{1(k_1)},x_{2(k_2)},\cdots,x_{R(k_R)}\right]\in\Omega_m}f'\left[x_{1(k_1)},x_{2(k_2)},\cdots,x_{R(k_R)}\right] \tag{74}$$

REFERENCES

[1] M. H. Barmayoon, M. Fotuhi-Firuzabad, A. Rajabi-Ghahnavieh, and M. Moeini-Aghtaie, "Energy storage in renewable-based residential energy hubs," *IET Generation Transmission & Distribution*, vol. 10, no. 13, pp. 3127-3134, 2016.

[2] S. Paudyal, C. A. Cañizares, and K. Bhattacharya, "Optimal Operation of Industrial Energy Hubs in Smart Grids," *IEEE Trans. Smart Grid*, vol. 6, no. 2, pp. 684-694, 2015.

[3] S. Bahrami, and A. Sheikhi, "From Demand Response in Smart Grid Toward Integrated Demand Response in Smart Energy Hub," *IEEE Trans. Smart Grid*, vol. 7, no. 2, pp. 650-658, 2016.

[4] D. W. Wu, and R. Z. Wang, "Combined cooling, heating and power: A review," *Progress in Energy & Combustion Science*, vol. 32, no. 5, pp. 459-495, 2006.

[5] H. Mu, L. Li, N. Li, and M. Li, "Analysis of the integrated performance and redundant energy of CCHP systems under different operation strategies," *Energy & Buildings*, vol. 99, pp. 231-242, 2015.

[6] A. Hawkes, and M. Leach, "Cost-effective operating strategy for residential micro-combined heat and power," *Energy*, vol. 32, no. 5, pp. 711-723, 2007.

[7] S. Mitra, L. Sun, and I. E. Grossmann, "Optimal scheduling of industrial combined heat and power plants under time-sensitive electricity prices," *Energy*, vol. 54, no. 2, pp. 194-211, 2013.

[8] M. Salimi, H. Ghasemi, M. Adelpour, and S. Vaez-Zadeh, "Optimal planning of energy hubs in interconnected energy systems: a case study for natural gas and electricity," *IET Generation Transmission & Distribution*, vol. 9, no. 8, pp. 695-707, 2015.

[9] A. Sheikhi, A. M. Ranjbar, and H. Oraee, "Financial analysis and optimal size and operation for a multicarrier energy system," *Energy & Buildings*, vol. 43, no. 1, pp. 71-78, 2011.

[10] F. Kienzle, P. Ahcin, and G. Andersson, "Valuing Investments in Multi-Energy Conversion, Storage, and Demand-Side Management Systems Under Uncertainty," *IEEE Trans. Sust. Energ.*, vol. 2, no. 2, pp. 194-202, 2011.

[11] M. Rastegar, M. Fotuhi-Firuzabad, H. Zareipour, and M. Moeini-Aghtaieh, "A Probabilistic Energy Management Scheme for Renewable-Based Residential Energy Hubs," *IEEE Trans. Smart Grid*, vol. 8, no. 5, pp. 2217-2227, 2017.

[12] M. C. Bozchalui, S. A. Hashmi, H. Hassen, C. A. Canizares, and K. Bhattacharya, "Optimal Operation of Residential Energy Hubs in Smart Grids," *IEEE Trans. Smart Grid*, vol. 3, no. 4, pp. 1755-1766, 2012.

[13] A. Vaccaro, C. Pisani, and A. F. Zobaa, "Affine arithmetic-based methodology for energy hub operation-scheduling in the presence of data uncertainty," *IET Generation Transmission & Distribution*, vol. 9, no. 13, pp. 1544-1552, 2015.

[14] S. Bahrami, M. Toulabi, S. Ranjbar, M. Moeini-Aghtaie, and A. M. Ranjbar, "A Decentralized Energy Management Framework for Energy Hubs in Dynamic Pricing Markets," *IEEE Trans. Smart Grid*, to be published.

[15] L. Ma, N. Liu, L. Wang, J. Zhang, J. Lei, Z. Zeng, C. Wang, and M. Cheng, "Multi-party energy management for smart building cluster with PV systems using automatic demand response," *Energy & Buildings*, vol. 121, pp. 11-21, 2016.

[16] W. Saad, Z. Han, and H. V. Poor, "Coalitional game theory for cooperative micro-grid distribution networks," in *IEEE International Conference on Communications Workshops*, 2011, pp. 1-5.

[17] W. Lee, L. Xiang, R. Schober, and V. W. S. Wong, "Direct Electricity Trading in Smart Grid: A Coalitional Game Analysis," *IEEE J. Sel. Areas Commun.* , vol. 32, no. 7, pp. 1398-1411, 2014.

[18] W. Fan, N. Liu, J. Zhang, and J. Lei, "Online air-conditioning energy management under coalitional game framework in smart community," *Energies*, vol. 9, no. 9, pp. 689, 2016.

[19] N. Liu, Q. Tang, J. Zhang, W. Fan, and J. Liu, "A hybrid forecasting model with parameter optimization for short-term load forecasting of micro-grids," *Appl. Energy* vol. 129, pp. 336-345, 2014.

[20] N. Liu, X. Yu, C. Wang, C. Li, L. Ma, and J. Lei, "Energy-Sharing Model With Price-Based Demand Response for Microgrids of Peer-to-Peer Prosumers," *IEEE Trans. Power Syst.* , vol. 32, no. 5, pp. 3569-3583, 2017.

[21] L. Ma, N. Liu, J. Zhang, W. Tushar, and C. Yuen, "Energy management for joint operation of CHP and PV prosumers inside a grid-connected microgrid: A game theoretic approach," *IEEE Trans. Ind. Inf.* , vol. 12, no. 5, pp. 1930-1942, 2016.

[22] J. Chen, X. Yang, L. Zhu, and M. Zhang, "Genetic algorithm based economic operation optimization of a combined heat and power microgrid," *Power Sys. Prot. Control.*, vol. 41, no. 8, pp. 7-15, 2013 (in Chinese).

[23] M. Houwing, R. R. Negenborn, and B. De Schutter, "Demand Response With Micro-CHP Systems," *Proc. IEEE,* vol. 99, no. 1, pp. 200-213, 2011.

[24] R. T. Rockafellar, and S. Uryasev, "Optimization of Conditional Value-At-Risk," *Journal of Risk*, vol. 29, no. 1, pp. 1071–1074, 2010.

[25] Z. Han, *Game theory in wireless and communication networks: theory, models, and applications*: Cambridge University Press, 2012.

[26] L. S. Shapley, "A value for n-person games," *Annals of Mathematics Studies*, vol. 2, no. 28, pp. 307-317, 1953.

[27] J. Xie, *Optimization Modeling and LINDO/LINGO Software*: Tsinghua University Press, 2005.

[28] B. M. Hodge, D. Lew, and M. Milligan, "Short-Term load forecast error distributions and implications for renewable integration studies," in *IEEE Green Technologies Conference*, 2013, pp. 435-442.

[29] J. Macqueen, "Some methods for classification and analysis of multivariate observations," in *Proc. of Berkeley Symposium on Mathematical Statistics and Probability*, 1967, pp. 281–297.

This article has been accepted for publication in a future issue of this journal, but has not been fully edited. Content may change prior to final publication. Citation information: DOI 10.1109/TPWRS.2018.2877236, IEEE Transactions on Power Systems

Li Ma received the B.S., M.S. and Ph.D. degrees in electric engineering from North China Electric Power University, Beijing, China, in 2008, 2011, 2017 respectively.

She worked in the China Electric Power Research Institute as an Engineer from 2011 to 2018. Currently, she is a Research Associate in the Department of Electrical Engineering and Computer Science, University of Wisconsin-Milwaukee, Milwaukee, Wisconsin, USA.

Her research interests include smart grid, game theory, and urban distribution network planning.

Nian Liu (S'06–M'11) received the B.S. and M.S. degrees in electric engineering from Xiangtan University, Hunan, China, in 2003 and 2006, respectively, and the Ph.D. degree in electrical engineering from North China Electric Power University, Beijing, China, in 2009.

From 2015 to 2016, he was a Visiting Research Fellow with RMIT University, Melbourne, Australia. Currently, he is an Associate Professor in the School of Electrical and Electronic Engineering of North China Electric Power University, Beijing, China. His research interests include demand side energy management, microgrids, electric vehicles, and cyber security of smart grid.

He serves as Associate Editor of Journal of Modern Power Systems and Clean Energy (MPCE), reviewers for more than 10 top-tier international and Chinese journals, and Technical Track Co-chair of IEEE IECON2017.

Jianhua Zhang (M'04) was born in Beijing, China, in 1952. He received the M.S. degree in electrical engineering from North China Electric Power University, Beijing, China, in 1984.

He was a Visiting Scholar with the Queen's University, Belfast, U.K., from 1991 to 1992, and was a Multimedia Engineer of Electric Power Training with CORYS T.E.S.S., France, from 1997 to 1998. Currently, he is a Professor and Head of the Transmission and Distribution Research Institute, North China Electric Power University, Beijing. He is also the Consultant Expert of National "973" Planning of the Ministry of Science and Technology. His research interests are in power system security assessment, operation and planning, and micro-grid.

Prof. Zhang is an IET Fellow and a member of several technical committees.

Lingfeng Wang (S'02--M'09--SM'18) received the B.E. degree in measurement and instrumentation from Zhejiang University, Hangzhou, China, in 1997; the M.S. degree in instrumentation science and engineering from Zhejiang University, Hangzhou, China, in 2000; the M.S. degree in electrical and computer engineering from the National University of Singapore, Singapore, in 2002; and the Ph.D. degree from the Electrical and Computer Engineering Department, Texas A&M University, College Station, TX, USA, in 2008. He is currently a Professor with the Department of Electrical Engineering and Computer Science, University of Wisconsin-Milwaukee, Milwaukee (UWM), WI, USA, where he directs the cyber-physical energy systems research group. He also serves as a Co-Director for the Department of Energy (DOE)'s Industrial Assessment Center. He was a faculty member with the University of Toledo, Toledo, OH, USA, and an Associate Transmission Planner with the California Independent System Operator, Folsom, CA, USA. His current research interests include power system reliability and resiliency, smart grid cybersecurity, critical infrastructure protection, energy-water nexus, renewable energy integration, intelligent and energy-efficient buildings, electric vehicles integration, microgrid analysis and management, and cyber-physical systems.

Prof. Wang is an Editor of the IEEE TRANSACTIONS ON SMART GRID, IEEE TRANSACTIONS ON POWER SYSTEMS, and IEEE POWER ENGINEERING LETTERS, and serves on the Steering Committee of the IEEE TRANSACTIONS ON CLOUD COMPUTING. He is also an Editorial Board Member for several international journals, including Journal of Modern Power System and Clean Energy, Sustainable Energy Technologies and Assessments, and Intelligent Industrial Systems. He served as a Co-chair for IEEE SmartGridComm'15 Symposium on Data Management, Grid Analytics, and Dynamic Pricing. He is a recipient of the Outstanding Faculty Research Award of College of Engineering and Applied Science at UWM in 2018.